



Research Paper

The manganese(III) porphyrin MnTnHex-2-PyP⁵⁺ modulates intracellular ROS and breast cancer cell migration: Impact on doxorubicin-treated cells

Ana Flório^{a,b,1}, Nuno Saraiva^{a,1}, Sara Cerqueira^a, Nuno Almeida^a, Maddy Parsons^c, Ines Batinic-Haberle^d, Joana P. Miranda^b, João G. Costa^{a,b}, Guia Carrara^e, Matilde Castro^b, Nuno G. Oliveira^{b,2}, Ana S. Fernandes^{a,*,2}

^a CBIOS, Universidade Lusófona Research Center for Biosciences & Health Technologies, Campo Grande 376, Lisboa 1749-024, Portugal

^b Research Institute for Medicines (iMed.Ulisboa), Faculty of Pharmacy, Universidade de Lisboa, Av. Professor Gama Pinto, Lisboa 1649-003, Portugal

^c Randall Centre for Cell and Molecular Biophysics, King's College London, London SE1 1UL, England, UK

^d Department of Radiation Oncology, Duke University School of Medicine, Durham, NC, USA

^e Department of Pathology, University of Cambridge, Cambridge CB2 1QP, UK



ARTICLE INFO

Keywords:

Cancer
Cell migration
Cell invasion
SOD mimics
Manganese porphyrins
Redox modulation

ABSTRACT

Manganese(III) porphyrins (MnPs) are superoxide dismutase (SOD) mimics with demonstrated beneficial effects in cancer treatment in combination with chemo- and radiotherapy regimens. Despite the ongoing clinical trials, little is known about the effect of MnPs on metastasis, being therefore essential to understand how MnPs affect this process. In the present work, the impact of the MnP MnTnHex-2-PyP⁵⁺ in metastasis-related processes was assessed in breast cancer cells (MCF-7 and MDA-MB-231), alone or in combination with doxorubicin (dox). The co-treatment of cells with non-cytotoxic concentrations of MnP and dox altered intracellular ROS, increasing H₂O₂. While MnP alone did not modify cell migration, the co-exposure led to a reduction in collective cell migration and chemotaxis. In addition, the MnP reduced the dox-induced increase in random migration of MDA-MB-231 cells. Treatment with either MnP or dox decreased the proteolytic invasion of MDA-MB-231 cells, although the effect was more pronounced upon co-exposure with both compounds. Moreover, to explore the cellular mechanisms underlying the observed effects, cell adhesion, spreading, focal adhesions, and NF-κB activation were also studied. Although differential effects were observed according to the endpoints analysed, overall, the alterations induced by MnP in dox-treated cells were consistent with a therapeutically favorable outcome.

1. Introduction

Superoxide dismutase mimics (SODm) are described as a group of synthetic compounds that possess the ability to mimic the functional properties of native superoxide dismutases. SODm are catalytical polyfunctional antioxidants, being thus effective not only in the disproportionation of superoxide anion but also in the elimination of other

reactive species [1]. Moreover, SODm may also interact with redox domains of several signaling proteins involved in cancer development [1]. Notably, SODm have repeatedly demonstrated beneficial effects in different *in vitro* and *in vivo* experimental models of several human pathologies, including cardiovascular, neurodegenerative, and inflammatory diseases as well as different types of cancer [2,3]. There is growing evidence that SODm have indeed several features that can be

Abbreviations: CAT, catalase; CV, crystal violet; DAPI, 4',6-diamino-2-phenylindole; DHE, dihydroethidium; DHR, dihydrorhodamine 123; DMEM, Dulbecco's Modified Eagle's Medium; DMSO, dimethylsulfoxide; dox, doxorubicin; ECM, extracellular matrix; EDTA, ethylenediaminetetraacetic acid; FA, focal adhesions; FAK, focal adhesion kinase; FBS, foetal bovine serum; GAPDH, glyceraldehyde 3-phosphate dehydrogenase; IB, immunoblotting; MnP, Manganese(III) porphyrin; MnTnHex-2-PyP⁵⁺, Mn(III) 5,10,15,20-meso-tetrakis(*N*-*n*-hexylpyridinium-2-yl)porphyrin (charges are omitted throughout the text for clarity); MMPs, matrix metalloproteinases; MnSOD, Manganese-superoxide dismutase (SOD2); MTT, 3-(4,5-dimethylthiazol-2-yl)-2,5-diphenyl-2H-tetrazolium bromide; NF-κB, nuclear factor kappa B; PBS, phosphate buffered saline; PFA, paraformaldehyde; PI, propidium iodide; ROS, reactive oxygen species; SDS, sodium dodecyl sulfate; SOD, superoxide dismutase; SODm, superoxide dismutase mimics; TNF-α, Tumor Necrosis Factor-α

* Corresponding author.

E-mail address: ana.fernandes@ulusofona.pt (A.S. Fernandes).

¹ Both authors equally contributed.

² Shared senior authorship.

<https://doi.org/10.1016/j.redox.2018.10.016>

Received 12 September 2018; Received in revised form 19 October 2018; Accepted 21 October 2018

Available online 25 October 2018

2213-2317/ © 2018 The Authors. Published by Elsevier B.V. This is an open access article under the CC BY-NC-ND license (<http://creativecommons.org/licenses/by-nc-nd/4.0/>).

valuable for cancer treatment. In this context, Manganese Porphyrins (MnPs) have been pointed out as one of the most promising classes of SODm [1]. We [4,5] have recently addressed the rationale for the use of SODm in cancer therapy. Due to the differential effects of SOD on nontumor vs tumor cells, several reports have demonstrated the usefulness of SODm, including MnPs, either as protectors of normal cells against radio- and chemotherapy or as prototype drugs to impair cancer cell proliferation. As a consequence, some SODm are currently being evaluated in cancer clinical trials, in combination with chemo- or radiotherapy regimens [1,4]. Despite all the evidences supporting a role for SODm in cancer therapy, the effect of such compounds in metastasis is still almost unexplored. It is accepted that ROS can regulate key cellular mechanisms involved in cancer cell migration/invasion, including invadopodia formation, MMP activation/expression, focal adhesion dynamics, cell-cell contact, cytoskeleton remodelling, and gene expression [4]. SODm may therefore also impact cancer metastasis.

Although elevating SOD enzymes levels generally inhibit tumor invasiveness, some reports show the opposite effect [6]. In the case of breast cancer, MnSOD can have a dual role in tumorigenic progression [5]. While at an early cancer stage MnSOD can work as a caretaker gene [7], the expression and activity levels of this enzyme have been shown to enhance breast cancer metastatic phenotype [8]. Considering this dual effect of SOD in breast cancer progression along with the previous *in vitro* and *in vivo* studies that suggest the potential use of SODm in breast cancer treatment [5], it is essential to explore the impact of SODm on cell processes related to metastases. This information will be important to exclude potential detrimental effects related to cell migration, in case of a future application of SODm in breast cancer treatment.

In this context, the present report addresses the effect of MnTnHex-2-PyP⁵⁺ (Fig. 1), a promising SODm [1] in human breast cancer cells with low (MCF7) and high (MDA-MB-231) aggressiveness. The innovative aspects of this work include the evaluation of the impact of the MnP in several types of cell migration in cells treated with doxorubicin (dox), a widely used chemotherapy drug for metastatic breast cancer. In the present report, SODm exhibited beneficial effects in reducing the migration of dox-treated cells. Furthermore, to explore the cellular mechanisms underlying the observed effects, several aspects related to the migratory phenotype were studied.

2. Material and methods

2.1. Chemicals

Dulbecco's Modified Eagle's Medium (DMEM), foetal bovine serum (FBS), penicillin-streptomycin solution, insulin solution from bovine pancreas, trypsin, 3-(4,5-dimethylthiazol-2-yl)-2,5-diphenyl-2H-tetrazolium bromide (MTT), crystal violet, dox, catalase (CAT), EDTA, PFA, RNase A, DAPI, glutaraldehyde (25% commercial solution), NaBH₄ and

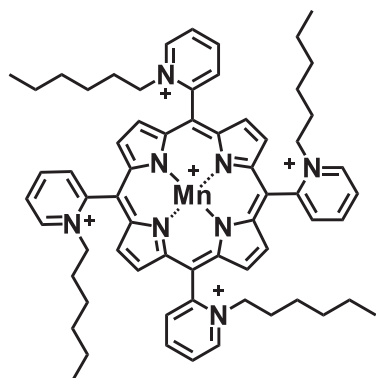


Fig. 1. Chemical structure of MnTnHex-2-PyP⁵⁺ [9].

TNF- α were purchased from Sigma-Aldrich (St Louis, MO, USA). Dimethylsulfoxide (DMSO), propidium iodide (PI), ethanol and acetic acid were purchased from Merck (Darmstadt, Germany). Acetic acid glacial and NaCl were purchased from Panreac (Barcelona, Spain). Matrigel™ was purchased from BD Biosciences (San Jose, CA, USA). Oregon Green 488-conjugated gelatin was acquired from Life Technologies (Oregon, USA). Dihydrorhodamine 123 (DHR) and dihydroethidium (DHE) probes were purchased from Molecular Probes (Eugene, OR, USA). For these probes, 10 mM stock solutions were prepared in DMSO, aliquoted and stored under nitrogen at -20°C . MnTnHex-2-PyP⁵⁺ was synthesized and characterized as described by Batinić-Haberle et al. [9]. Mowiol 4-88 and antibodies anti-vinculin, anti-FAK and anti-Tubulin were obtained from EMD Millipore (Burlington, Massachusetts, USA). NuPAGE®Novex 4–12% Bis-Tris gels, primary antibody anti-pFAK Y397 and secondary antibody conjugated to Alexa Fluor 488 were obtained from Invitrogen (Grand Island, NY, USA). Antibodies anti-Paxillin and anti-GAPDH were obtained from Cell Signaling Technology (Danvers, MA, USA). RIPA buffer was purchased from Roche (Basel, Switzerland). pTK-Renilla luciferase and passive lysis buffer 5X were obtained from Promega (Madison, WI, USA). Lipofectamine® LTX Reagent and PLUSTM Reagent were purchased from ThermoFisher Scientific (Carlsbad, California, USA).

2.2. Cell culture

Human breast cancer cell lines MDA-MB-231 and MCF7 were obtained from ATCC and DSMZ, respectively. Both cell lines were kept in DMEM supplemented with 10% FBS, 100 U/mL penicillin and 0.1 mg/mL streptomycin. MCF7 cells medium was additionally supplemented with 0.1% insulin. Cultures were kept at 37°C , under a humidified atmosphere containing 5% CO₂.

2.3. Cell viability assay

The effect of MnTnHex-2-PyP in cell viability, either given alone or in combination with dox, was determined by the MTT assay. Briefly, 6.5×10^3 cells (for MCF7) or 5×10^3 cells (for MDA-MB-231) were cultured in 200 μL of complete medium in 96-well plates. The cells were grown for 48 h and then exposed to different concentrations of dox (0.5–5 μM for MCF7 cells and 0.5–20 μM for MDA-MB-231 cells), alone or in combination with MnTnHex-2-PyP (5 μM), for a 24 h-period. MTT reduction assay was performed as previously described by Fernandes et al. [10]. Two to ten independent experiments were performed, and four replicate cultures were used for each condition.

2.4. Cell cycle analysis

The effect of MnTnHex-2-PyP on cell cycle distribution and cell death was analysed by PI staining of fixed cells. MDA-MB-231 and MCF7 cells were seeded in 6-well plates in complete growth medium. Twenty-four h later cells were exposed to vehicle, dox (0.1 μM), MnTnHex-2-PyP (5 μM), or both drugs for 16 h at 37°C in complete medium. Both floating and adherent cells were collected using 5 mM EDTA in PBS. Cells were washed with cold PBS and fixed with cold 80% ethanol. Cells were resuspended in PBS with 1% FBS and after RNase A-treatment (50 $\mu\text{g}/\text{mL}$; Sigma-Aldrich, St Louis, MO, USA) and PI (25 $\mu\text{g}/\text{mL}$) staining for 15–20 min, cell DNA content was analysed using a FACSCalibur flow cytometer (BD). Data acquisition and analysis were performed using CellQuest software (BD) and FlowJo (Tree Star, San Carlos, Calif.), respectively.

2.5. Intracellular ROS measurement

The intracellular ROS levels were assessed by fluorescence microscopy using two different probes: dihydroethidium (DHE) and dihydrorhodamine 123 (DHR) [11,12]. For ROS assays, MDA-MB-231 and

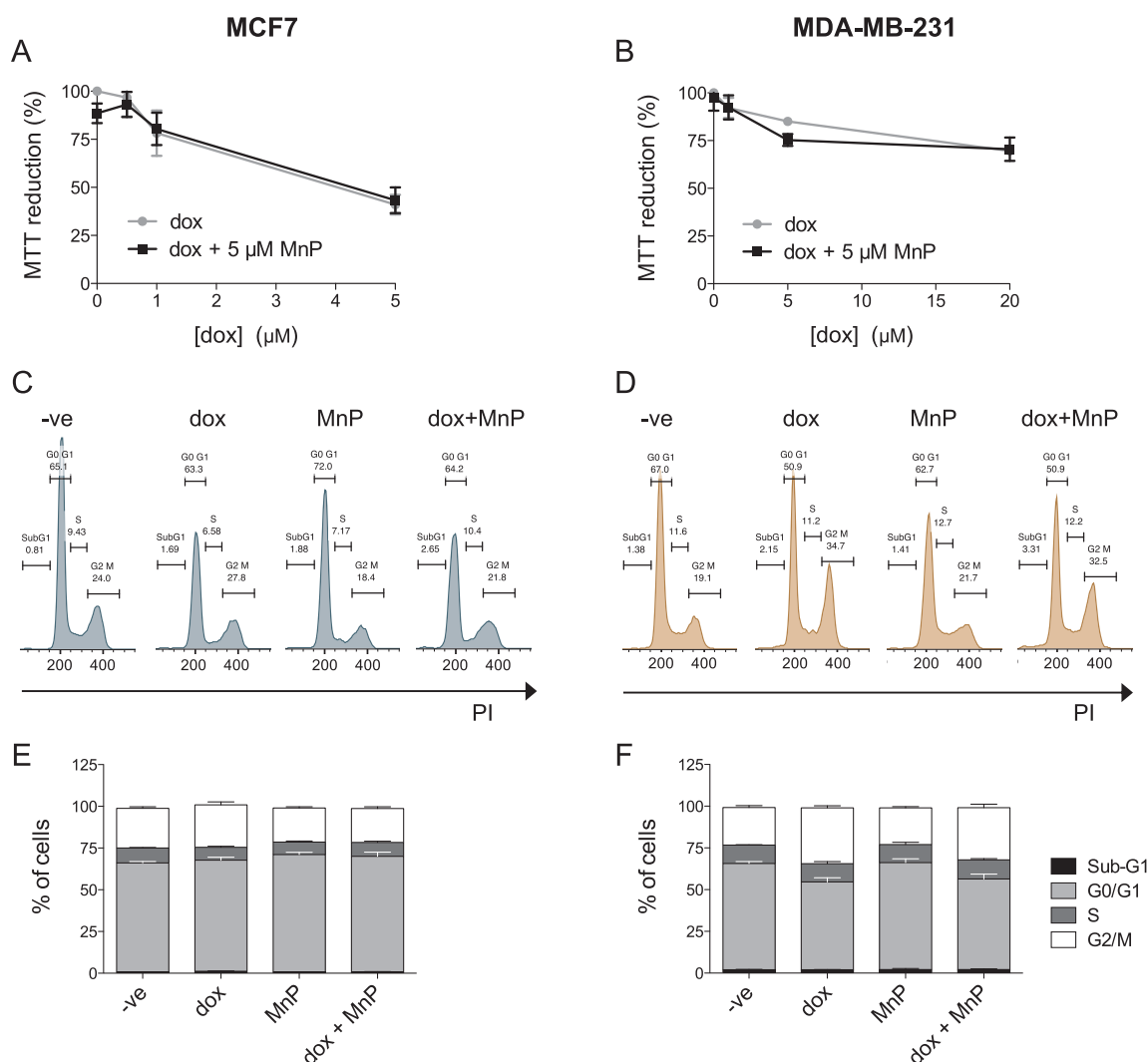


Fig. 2. Treatment with MnP and low concentrations of dox does not induce cell death. MCF7 (A, C and E) and MDA-MB-231 (B, D and F) cell viability and cell death induction following exposure to the indicated MnP and dox concentrations, were evaluated by an MTT assay (A and B) and a DNA content assay after cell fixation (C–F), respectively. Histograms show representative MCF7 and MDA-MB-231 DNA content profiles following exposure to dox (0.1 μM), MnP (5 μM) or both, fixation and PI stain (C–D). Summary results from cell viability (A and B) and DNA content assays (E and F) are represented as means ± SD. PI, propidium iodide.

MCF7 cells were seeded on Matrigel™-coated (1/30 dilution in FBS-free medium) dishes and after 24 h, when cells were ~40% confluent they were incubated with vehicle, dox (0.1 μM), MnTnHex-2-PyP (5 μM) or both drugs for 1 or 16 h at 37 °C in FBS-free medium. For the DHR assays, CAT (50 U/mL) was used alone or in combination with both drugs. Cells were then washed with warm PBS and incubated with DHR or DHE (10 μM) in FBS-free medium for 25 min at 37 °C. Cell image acquisition was performed using a wide field BX51 fluorescent Olympus microscope with a 40x objective using a 460–490 nm/ < 520 nm excitation/emission filter for DHR and a 520–550 nm/ < 580 nm excitation/emission filter for DHE. Cell fluorescence and area were determined using ImageJ (National Institutes of Health) [13] for a minimum of 45 cells per condition. Three to four independent experiments were performed.

2.6. In vitro wound-healing assay

The in vitro wound-healing assay was optimized according to Liang et al. [14]. MCF7 cells and MDA-MB-231 cells were seeded in 24-well plate with an inoculum of 2×10^5 cells per well and cultured in complete media for 24 h. After 24 h, media was removed, and each well was scratched using a 200 μL pipette tip, leaving a gap of approximately

0.8 mm in width. Cells were washed twice with PBS to remove detached cells and cell debris. Cells were kept in FBS- and insulin-free media containing the test compounds. The distance between the two limits of the scratch was monitored using a Motic AE 2000 inverted microscope with an objective of 10 × at 0 and 24 h after compounds addition. Images were collected using a Moticam 2500 and measurements were performed using Motic Images Plus V2.0 software. Zero h was considered as 0% of wound closure. At each time point one photo of each scratch was taken and three representative measures were performed. Each assay was performed with intern triplicates and at least 4 independent experiments were performed per condition.

2.7. Chemotaxis and chemoinvasion assays

The chemotactic migration of MCF7 and MDA-MB-231 cells was evaluated in 24-well plates with transwell inserts with transparent PET membranes containing 8 μm pores (BD Falcon, USA). Cells (1×10^5 cells in 200 μL of FBS-free medium) were seeded on the top of the insert and complete medium was placed in the lower chamber of the culture well. The test compounds were added to both chambers and cultures were incubated for 16 h. Non-migrating cells were removed from the upper side of the inserts with a cotton swab. Cells that migrated to the

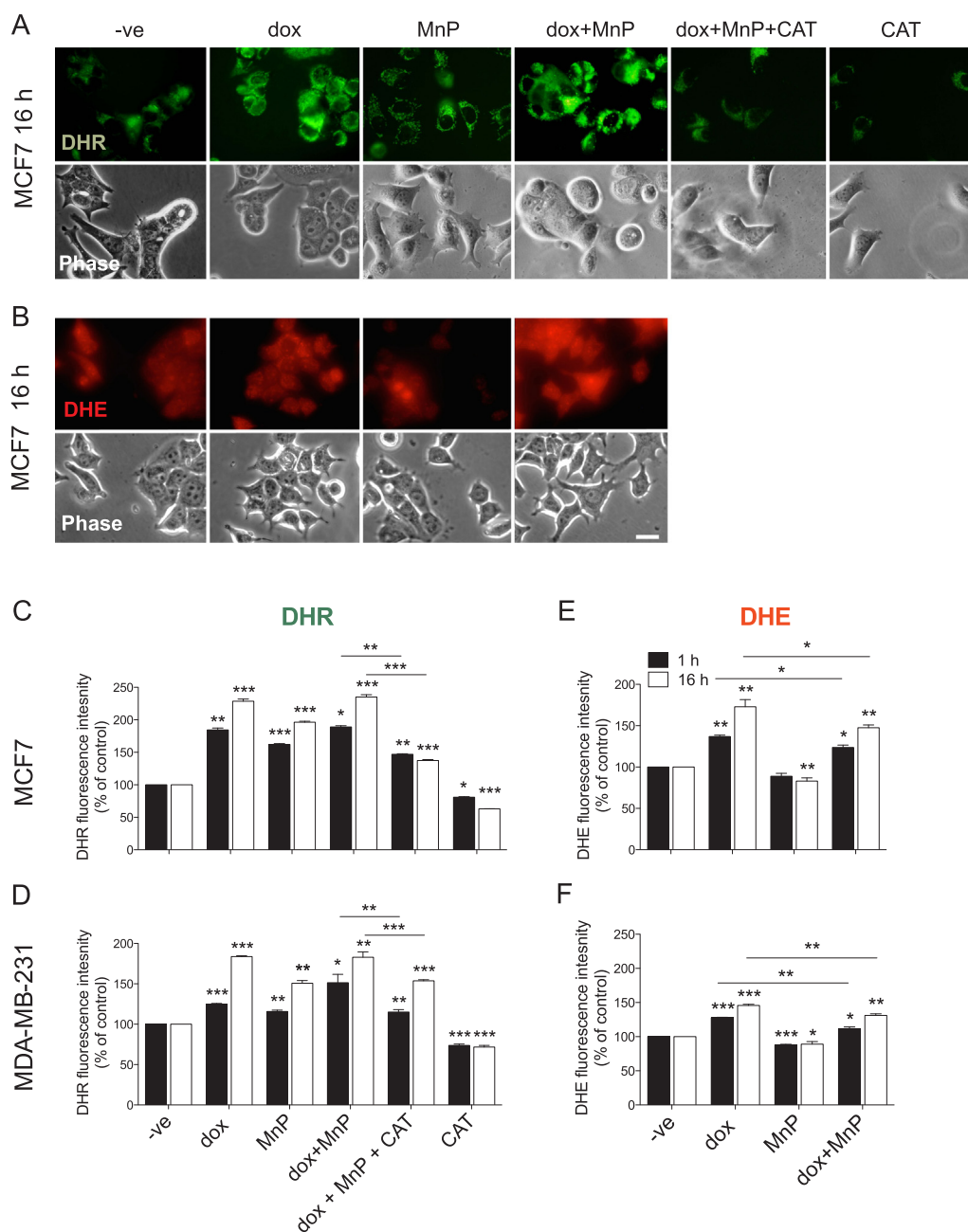


Fig. 3. MnP and dox lead to an increase in intracellular ROS. Intracellular ROS levels were determined in MCF7 (A, B, C and E) or MDA-MB-231 (D and F) cells treated with the indicated drugs (dox (0.1 μ M), MnP (5 μ M)). Fluorescence microscopy images show representative MCF7 cells after 25-min incubation with DHR and DHE (A and B). Scale bars = 20 μ m. Summary results (means \pm SD from at least three independent experiments) show relative DHR and DHE fluorescence (C to F). * p < 0.05, ** p < 0.01, *** p < 0.001 (one-way ANOVA with Tukey's test, relative to untreated cells).

underside of the inserts were fixed with cold 96% ethanol and stained with 0.1% CV in 10% ethanol. CV was resuspended in 96% ethanol with 1% acetic acid and the absorbance at 595 nm was measured in a Thermo Fisher Multiskan FC microplate reader. Three to five independent experiments were performed.

The chemoinvasion assay was performed as described for chemotaxis measurements, but herein the membrane filter was overlaid with Matrigel™ diluted in serum-free medium (1/30), which blocked non-invasive cells from migrating through [15,16]. Three to five independent experiments were performed.

2.8. Random cell migration assay

Individual random cell migration of MDA-MB-231 and MCF7 cells

was evaluated by time-lapse microscopy as previously described by Saraiva et al. [17]. Briefly, MDA-MB-231 or MCF7 cells were seeded at low density (30% confluent) on Matrigel™-coated 12-well plates. Drugs were added, and cells were allowed to adhere for 4 h at 37 °C. Individual cells were imaged at 10-min intervals for 12 h with a wide-field microscope (Observer. Z1; CarlZeiss) contained within an environmental chamber at 37 °C using a 10 \times objective and a camera (AxioCam HRm; Carl Zeiss). Migration tracks were generated using the ImageJ Manual Tracking plugin, and tracks were analysed using an in house-written Mathematica 7 notebook (provided by G. Dunn, King's College London, London, England, UK) to calculate migration rates and persistence.

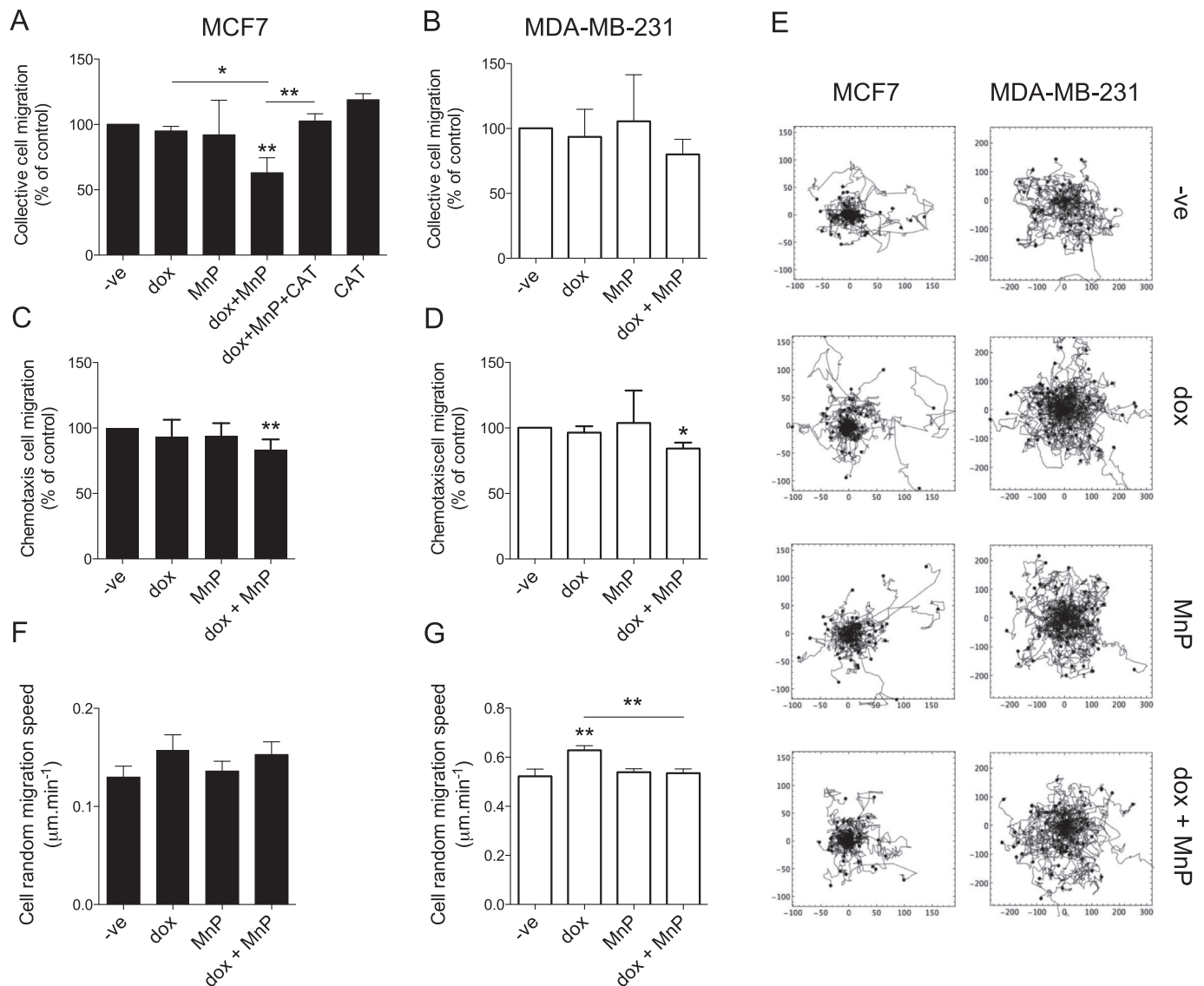


Fig. 4. MnP and dox can reduce chemotaxis and random and collective cell migration. Collective cell migration, chemotaxis and random migration of MCF7 (A, C and F) or MDA-MB-231 (B, D and G) cells treated with the indicated drugs (dox (0.1 μM), MnP (5 μM)) were measured. Collective cell migration was measured by the wound healing assay (A and B), chemotaxis was measured using a transwell system with FBS as chemoattractant (C and D) and random cell migration on matrigel was measured using time lapse microscopy (F and G). Tracks of individual migrating cells ($n = 60$ for each condition) used to measure random cell migration are shown in E. Migration rates (A–D and F–G) are shown as means \pm SD. * $p < 0.05$, ** $p < 0.01$ (Student's *t*-test, relative to untreated cells).

2.9. Gelatin degradation assay

Fluorescent gelatin-coated cover slips were prepared as described by Martin et al. [18]. Briefly, coverslips were coated with thin layers of Oregon Green 488-conjugated gelatin, cross-linked with 0.5% glutaraldehyde for 15 min, incubated for 3 min at room temperature with 5 mg/mL NaBH_4 and washed three times with PBS and incubated for 15 min in 70% ethanol. Cells were seeded on gelatin-coated coverslips at a density of 4×10^4 cells per well in complete DMEM and incubated with the relevant compounds. After 16 h cells were fixed in 4% PFA. Analysis was performed on a wide field BX51 fluorescent Olympus microscope with a $40 \times$ objective. The gelatine degradation percentage (per image) was measured using Image J software and was then normalized to the number of cells to obtain normalized degradation value.

2.10. Cell detachment assay

Cell detachment was analysed using an EDTA-induced cell detachment assay as previously described by Saraiva et al. [17]. Briefly, MDA-

MB-231 or MCF7 cells were seeded in 24-well plates for 24 h until cells reached $\sim 30\%$ confluency. Cells were incubated with vehicle, dox (0.1 μM), MnTnHex-2-PyP (5 μM) or both drugs for 24 h, at 37 $^\circ\text{C}$ in complete cell culture medium. After treatment, cells were washed with PBS, incubated with PBS-EDTA (1 mM) or cell media for 10 min at 37 $^\circ\text{C}$ and washed with PBS to remove non-adherent cells. The remaining adherent cells were fixed using 4% PFA and stained with 0.1% CV in 10% ethanol. The wells were washed with water, and the dye was eluted using 1% acetic acid in 96% ethanol. Absorbance was measured at 595 nm on a Multiskan FC (Thermo Fisher Scientific) microplate reader. Three independent experiments were performed.

2.11. Cell spreading assay

Cell spreading evaluation was performed similarly as previously described by Saraiva et al. [17]. MDA-MB-231 and MCF7 cells were detached with trypsin, resuspended in complete medium and incubated for 30 min or 16 h with the appropriate drugs. Cells were seeded in MatrigelTM-coated coverslips and left to attach for 20 min, 35 min and

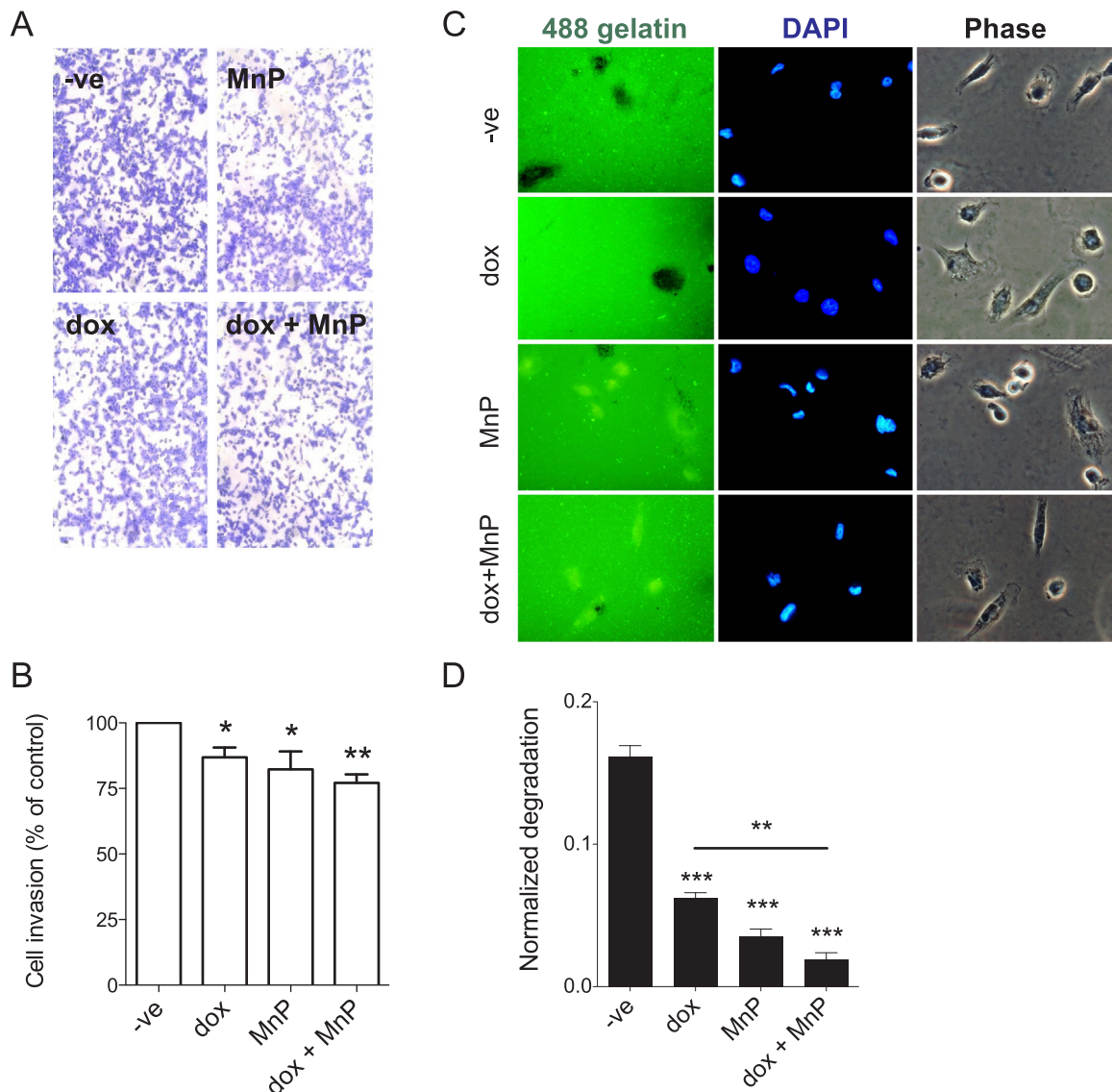


Fig. 5. Treatment with MnP and dox reduces MDA-MB-231 cell invasion and extracellular proteolytic activity. MDA-MB-231 cells were seeded on matrigel-coated transwells and were allowed to invade for 16 h in the presence of the indicated drugs (dox (0.1 μ M), MnP (5 μ M)) (A). The percentage of invading cells is summarized in B. The extracellular proteolytic activity was measured using a fluorescent gelatine degradation assay (C). Invasion rates (B), and normalized gelatine degradation (D) from at least three independent experiments are shown as means \pm SD. * p < 0.05, ** p < 0.01, *** p < 0.001 (Student's t -test, relative to untreated cells).

12 h or 3 h and 12 h, for MDA-MB-231 and MCF7, respectively. Cells were fixed with 4% PFA, washed with PBS and the coverslips were mounted in Mowiol 4–88 containing DAPI. Image acquisition was performed with a wide field BX51 fluorescent Olympus microscope with a 40 \times objective. Cell area was determined using Image J. Mean cell areas were normalized to the untreated control at 12 h. Three independent experiments were performed for each protocol.

2.12. Focal adhesion number

MDA-MB-231 or MCF7 cells were seeded in Matrigel™ –coated coverslips so that they would reach 30–40% confluence 40 h later. Drugs were added to cells 24 h post seeding and were left to incubate for another 16 h. Cells were fixed with 4% PFA and stained with anti-pFAK Y³⁹⁷ (1:80) and with secondary antibodies conjugated to Alexa Fluor 488. Coverslips were mounted in Mowiol 4–88 containing DAPI. Cells were imaged by confocal microscopy using a 63 \times oil objective and a microscope (LSM 5 Pa; Carl Zeiss). Images were acquired using LSM image browser software (Carl Zeiss) and the number of focal adhesions per cell was counted.

2.13. Immunoblotting

The expression and phosphorylation of focal adhesion proteins (pFAK, FAK, paxilin, vinculin, GAPDH and tubulin) was evaluated by immunoblot. Briefly MDA-MB-231 or MCF7 cells were seeded in a Matrigel™-coated 12 well plate. Drugs were added to cells at 80% confluence and were left to incubate for 16 h. Cells were lysed with RIPA buffer (50 mM Tris pH 7.5, 500 mM NaCl, 0.5 mM MgCl₂, 0.1% Triton X-100, 0.1% SDS, 0.5% sodium deoxycholate, 1 mM EDTA, protease and phosphatase inhibitor cocktails). The lysates were cleared by centrifugation (15,000 \times g, 15 min), resolved using NuPAGE® Novex 4–12% Bis-Tris gels, and transferred onto a nitrocellulose membrane. Antigen-antibody complexes were detected and quantified using RDye-conjugated secondary antibodies and a LI-COR scanner (Odyssey). The primary antibodies used were: anti-pFAK Y³⁹⁷ (1:800), anti-FAK (1:1000), anti-Paxillin (1:2500), anti-Vinculin (1:1000), anti-GAPDH (1:5000) and anti-Tubulin (1:7500). Band intensity was quantified from three independent assays.

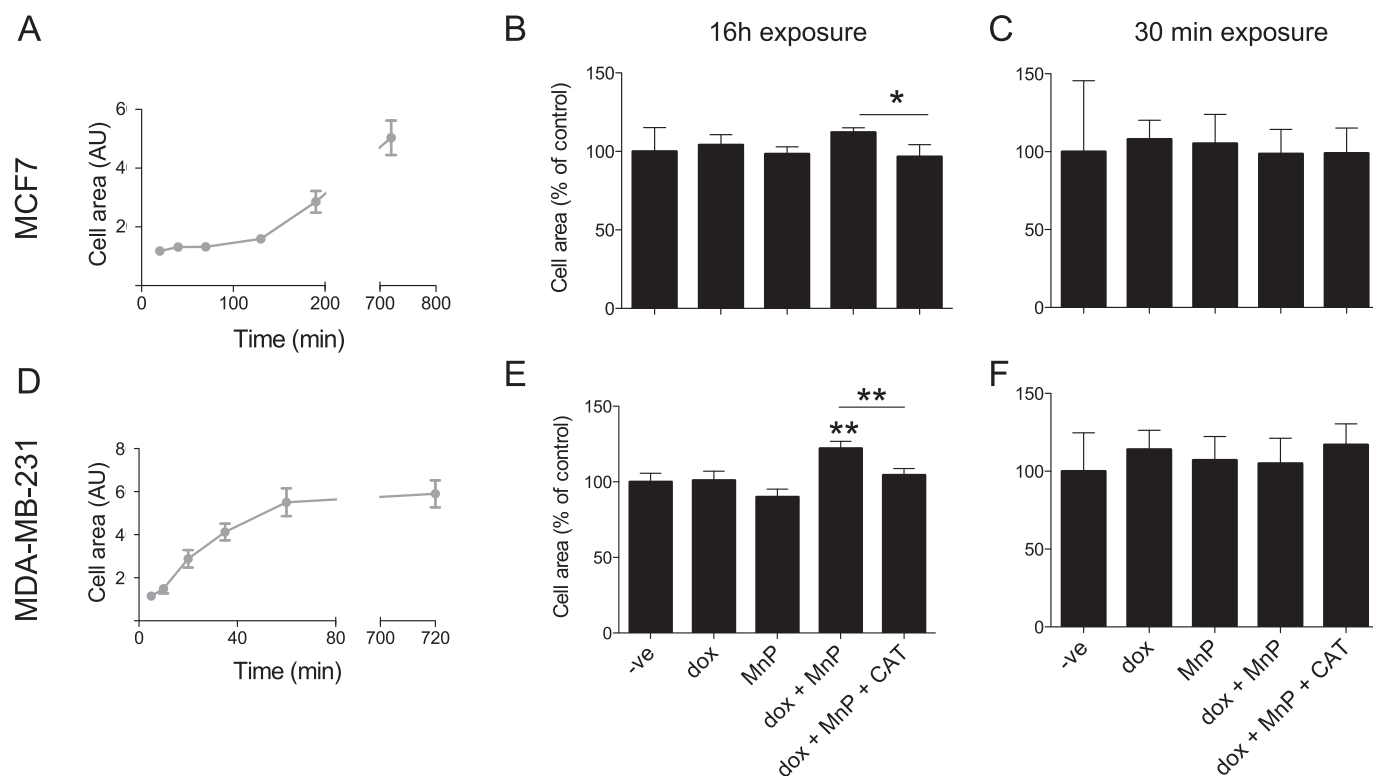


Fig. 6. Co-treatment with MnP and dox increases cell area. MCF7 and MDA-MB-231 cell spread on matrigel was monitored over time (A and D). Cells treated with the indicated drugs for 16 h (B and E) or 30 min (C and F) were seeded on matrigel-coated transwells and allowed to spread. The cells were left to adhere for 12 h and cell area was measured. Data is summarized in B, C, E and F. Cell area determined from at least three independent experiments ($n > 50$ cells per condition and per experiment) and are shown as means \pm SEM. * $p < 0.05$, ** $p < 0.01$ (one-way ANOVA with Tukey's test, relative to untreated cells).

2.14. NF- κ B gene reporter assay

Cells in 96-well plates were transfected with 60 ng/well of firefly luciferase NF- κ B reporter plasmid and 20 ng/well of pTK-Renilla luciferase (pRL-TK) as transfection control, using Lipofectamine[®] LTX Reagent and PLUSTM Reagent, according to the manufacturer's protocol. The plasmid encoding NF- κ B-firefly luciferase was a gift from R. Hofmeister (University of Regensburg, Germany). Forty-eight hours after transfections cells were treated for 16 h with the appropriate drugs and lysed using Passive Lysis Buffer. The relative stimulation of reporter-gene expression was calculated by normalizing firefly luciferase activity with renilla luciferase activity (both measured using a Synergy[™] HTX Multi-Mode Microplate Reader). In all cases, data shown are representative from at least three independent experiments, each comprising five replicates. TNF- α (50 ng/mL) was used as positive control.

3. Results

3.1. Impact of MnTnHex-2-PyP and dox on cell viability and cell death

The effect of MnTnHex-2-PyP and dox on the viability of human mammary cells was evaluated by the MTT assay (Fig. 2A and B). The MnP alone, at the biologically relevant concentration of 5 μ M [19] was not considerably toxic to MCF7 and MDA-MB-231 cells. Dox exhibited a concentration-response decrease in cell viability in both cell lines. However, MDA-MB-231 cells were more resistant to dox toxicity. For example, under our experimental conditions, exposure to 5 μ M of dox decreased cell viability more drastically in MCF7 than in MDA-MB-231 cells ($p < 0.001$). Dox cytotoxicity was not altered by the addition of MnTnHex-2-PyP (5 μ M). Cell viability studies allowed the identification of non-toxic levels of the compounds. The use of clinically relevant [20,21] and non-cytotoxic concentrations is essential when testing

potential inhibitors of migration/invasion [16,22]. Concentrations of 0.1 μ M of dox and 5 μ M of the MnP were selected for the subsequent experiments. To confirm that these concentrations did not induce cell death, the percentage of cells in sub-G1 was investigated. No differences were found in the Sub-G1 population in either cell line treated for 16 h with 0.1 μ M of dox and/or 5 μ M of the MnP (Fig. 2C–F). The cell cycle distribution was similar in MnP-treated and in control cells. However, MDA-MB-231 cells treated with dox presented a G2/M population increase (** $p < 0.001$), consistent with previous reports [23].

3.2. MnTnHex-2-PyP and dox modulate intracellular ROS levels

Since the biological effects of the MnP are probably associated with the modulation of the cellular redox status, the impact of the drugs in the intracellular levels of ROS was assessed using the DHE and DHR probes, after 1 or 16 h of drug exposure. DHE is a cell permeable probe that reacts with $O_2^{\cdot -}$ to form the fluorescent product 2-hydroxyethidium [24]. The oxidation of DHE is mostly superoxide-dependent and is considered to be quite insensitive to H_2O_2 [10,25,26]. DHR is widely used to evaluate general RS formation, and it is reactive with H_2O_2 in peroxidase-containing cells [24,27]. MCF7 and MDA-MB-231 cells incubated with dox, MnP or both drugs, exhibited a significant increase in ROS levels assessed by the DHR probe, which was more pronounced after 16 h of drug exposure. Catalase counteracted the increased ROS levels caused by the co-treatment with dox and MnP (Fig. 3A, C, D), demonstrating that higher ROS was in part due to enhanced H_2O_2 accumulation. DHE fluorescence was significantly increased in dox-treated cells, in both cell types and both incubation periods, and this was partially reverted by MnP (Fig. 3B, E, F), suggesting an increase in $O_2^{\cdot -}$ in dox-treated cells, as previously described [22,25,28]. The intracellular ROS alterations induced by the treatments were similar in both cell lines.

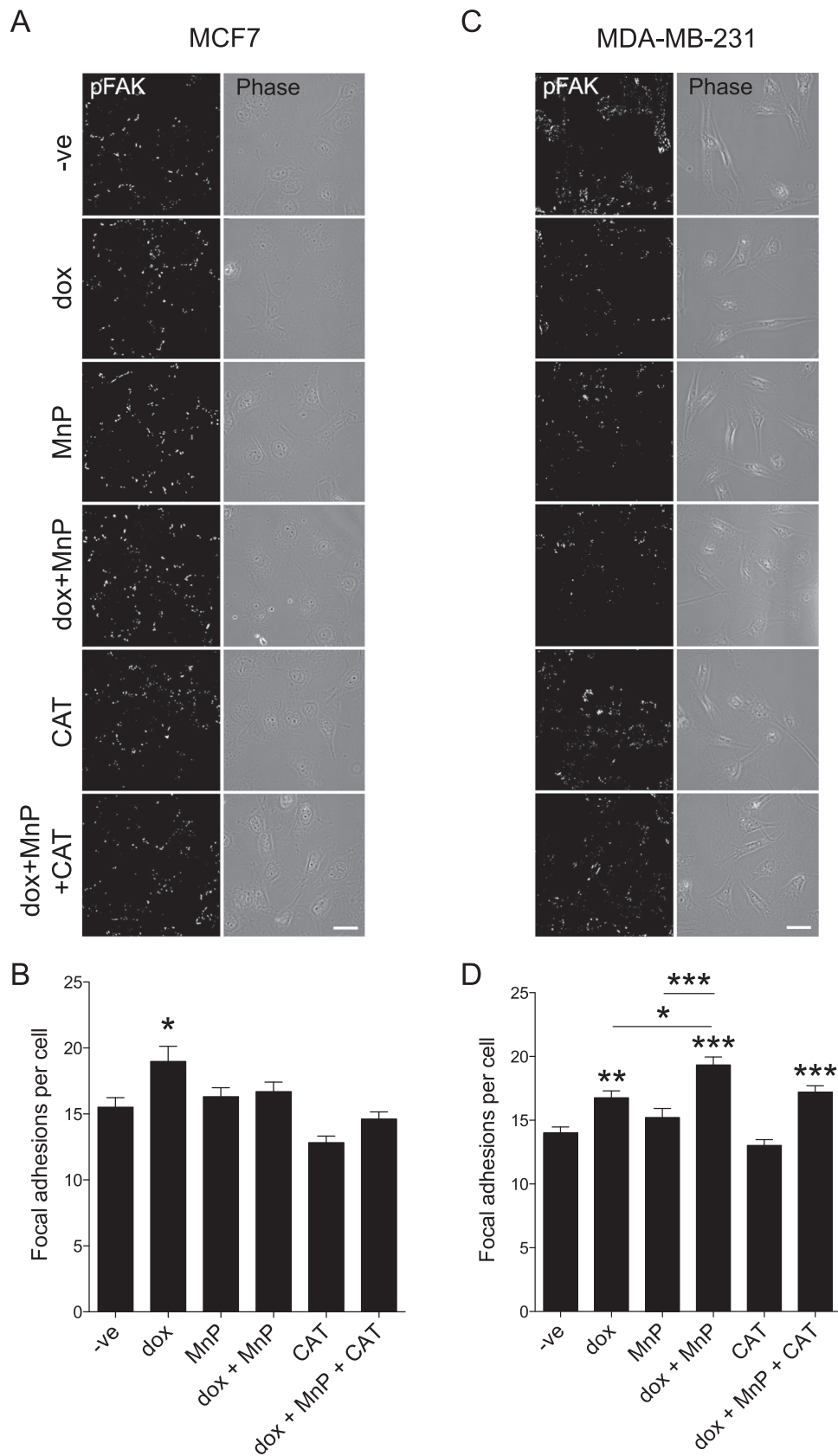


Fig. 7. Effect of MnP and dox on the number of focal adhesions. Confocal images show MCF7 (A) and MDA-MB-231 (C) cells treated with the indicated drugs for 16 h, fixed and stained with anti pFAK. Images are typical of three independent experiments. Scale bars, 20 μ m. Summary results (means \pm SEM from \geq 90 cells for each condition) show numbers of focal adhesions per cell, determined by counting pFAK positive spots (B and D). * $p < 0.05$, ** $p < 0.01$, *** $p < 0.001$ (one-way ANOVA with Tukey's test, relative to untreated cells).

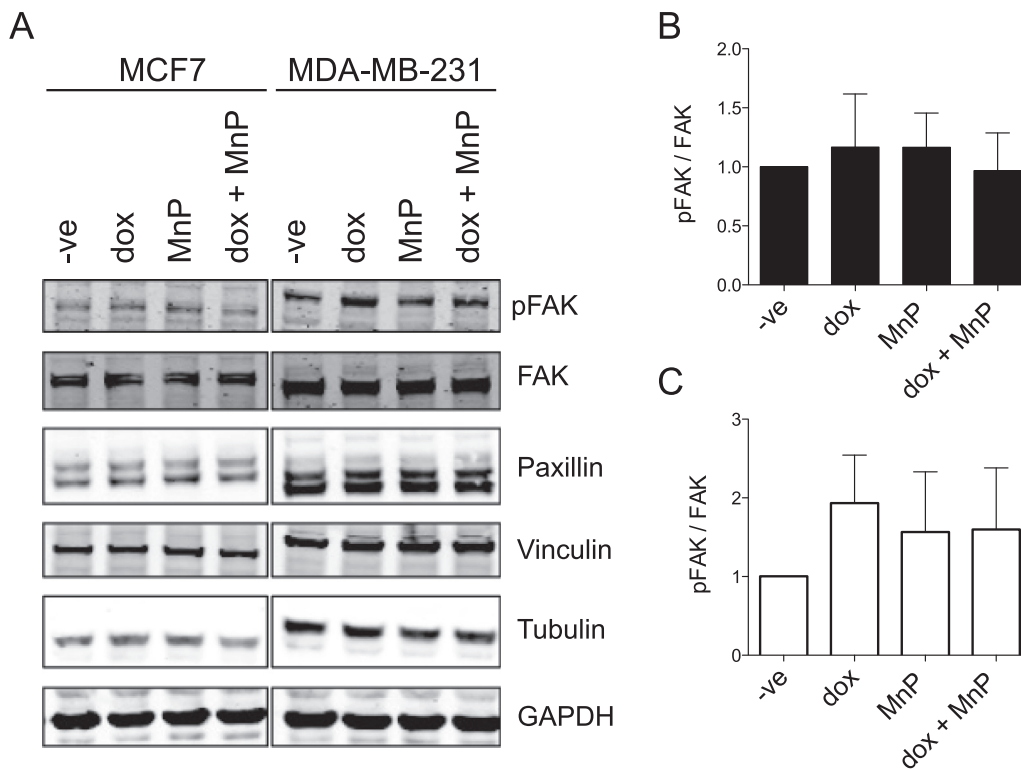


Fig. 8. Effect of MnP and dox treatment on the levels of FA proteins. Typical IB showing total pFAK, FAK, Paxillin and Vinculin and the loading controls (GAPDH and Tubulin) for MCF7 and MDA-MB-231 cells treated with the indicated drugs for 16 h (A). Summary results (means \pm SD from three independent experiments) show relative protein expression levels for MCF7 cells (B) and MDA-MB-231 cells (C).

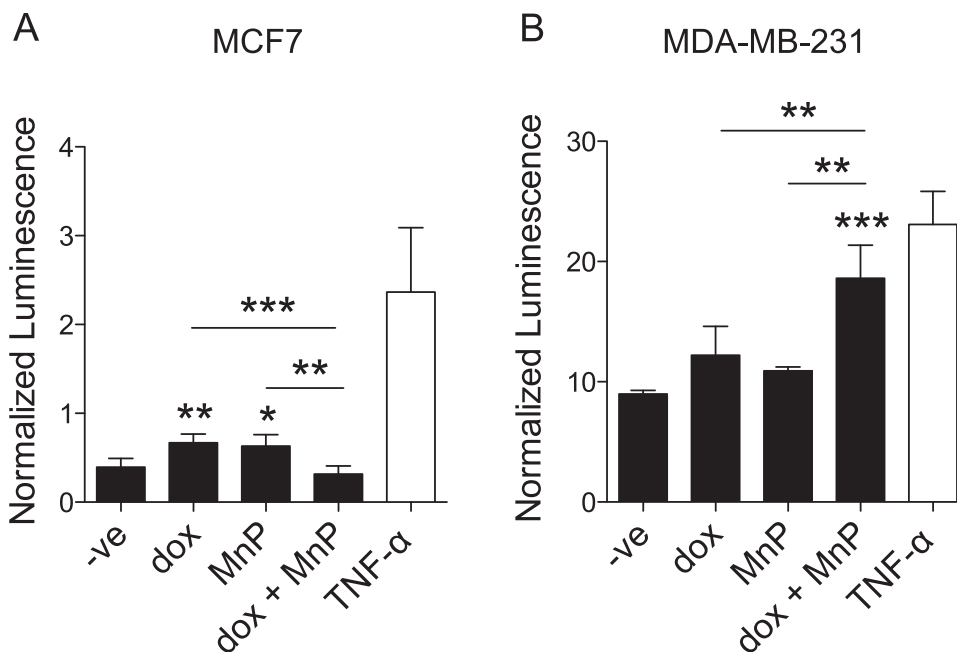


Fig. 9. Effect of MnP and dox treatment on NF- κ B-dependent transcription. MCF7 (A) and MDA-MB-231 (B) cells transfected with a firefly luciferase reporter plasmid under the control of an NF- κ B-dependent promoter and a renilla luciferase transfection control were treated with the indicated drugs for 16 h. Data are from one experiment representative of at least three, each performed in 5 replicates are presented as means \pm SD, * p < 0.05; ** p < 0.01; *** p < 0.001 (one-way ANOVA with Tukey's test), compared with untreated cells (-ve).

3.3. Impact of MnTnHex-2-PyP and dox on cell migration

Three different assays were used to evaluate the impact of dox and MnP on cell migration. Collective cell migration was assessed by wound-healing assays (Fig. 4A, B). While dox and MnP given alone did not significantly change cell migration, co-treatment led to a reduction in cell motility. This decrease was more pronounced in MCF7 cells, in which the % of wound closure decreased to $63 \pm 9\%$ of control.

To explore if H₂O₂ increased levels are associated with the reduction of collective cell migration observed upon the co-treatment with dox + MnP, experiments using CAT were performed. The addition of CAT reverted this inhibitory effect of dox + MnP (Fig. 4A), suggesting a role

for H₂O₂ in mediating this migration phenotype. Chemotaxis was evaluated by a transwell assay using FBS as chemoattractant. In both cell types, MnP or dox alone did not alter chemotaxis. However, simultaneous exposure to both compounds resulted in a significant decrease in chemotactic migration of MCF7 and MDA-MB-231 cells to $83.4 \pm 7.9\%$ and to $84.3 \pm 4.4\%$ of controls, respectively (Fig. 4C, D). Single cell random migration was also evaluated by time-lapse microscopy. As expected, the migration speed of MDA-MB-231 cells was higher than that of MCF7 cells (Fig. 4E–G, p < 0.001). While the drug treatments did not significantly change the random migration speed of MCF7 cells (Fig. 4E–F), dox promoted the migration of MDA-MB-231 cells (p < 0.01 versus control). This increase was reverted by the

addition of MnP (Fig. 4E, G). In the different conditions tested, no changes in migration persistence were observed (data not shown).

As the drug treatments influenced cell migration, the impact on cell adhesion/detachment was also determined. This was assessed by an EDTA-induced cell detachment assay, using experimental conditions that induced ~50% cell detachment in non-treated cells. Although no significant differences were found, the same trend was observed in MCF7 and MDA-MB-231 cells. While dox and the MnP did not change cell detachment, the co-exposure slightly reduced it (non-significant; data not shown).

3.4. Dox and MnTnHex-2-PyP reduce MDA-MB-231 cell invasion

Since a critical feature of metastatic cancer cells is their ability to invade tissues, the effect of the MnP and dox in cell invasion was evaluated. These experiments were only carried out with MDA-MB-231 cells, due to the non-invasive phenotype of MCF7 cells [29] (no invasion was observed under our experimental conditions; data not shown). Cell invasion was assessed using a transwell assay using FBS as a chemoattractant. Treatment with dox and MnP individually led to a significant decrease in cell invasion. The co-treatment with both drugs decreased cell invasion to $77.3 \pm 3.1\%$ of controls (Fig. 5A, B).

The invasion of cancer cells can be due to proteolytic degradation of ECM or from amoeboid cell migration through the ECM components [30]. Therefore, a gelatin degradation assay was performed to explore the contribution of the proteolytic degradation of ECM to the reduction in cell invasion observed. Treatment with dox or with MnP significantly reduced gelatin degradation to 38.4% and 21.7% of controls, respectively. The result obtained for dox is in accordance with previous data [31]. Treatment with both drugs together had a significantly greater impact on degradation inhibition (11.8% of control; Fig. 5C–D).

3.5. Impact of MnTnHex-2-PyP and dox on cell spreading

As the combination of dox with MnP influenced cell movement, further studies were carried out to explore the mechanisms underlying such effects. The analysis of cell spreading provides a simple experimental approach to determine general functional impacts on cytoskeletal assembly. As shown in Fig. 6A and D, MDA-MB-231 exhibited more rapid increase in cell area over time following plating as compared to MCF7 cells, suggesting more rapid cytoskeletal dynamics and focal adhesion turnover, which is compatible with the more migratory phenotype of these cells. However, exposure to MnP and/or dox had no effect on the cell spreading dynamics (data not shown).

Cells incubated with dox, MnP or both drugs for 30 mins also showed no difference in spread cell area (Fig. 6C, F). Conversely, a 16 h co-exposure to dox and MnP led to an increase in cell area in MDA-MB-231 cells, but not MCF7 ($p < 0.05$, when the impact of dox + MnP in the two cell lines is compared). This increase in cell area was significantly reverted by CAT (Fig. 6B, E), suggesting that H_2O_2 participates in dox + MnP-induced cell spreading.

3.6. Impact of MnTnHex-2-PyP and dox on focal adhesions number

Considering the differences in cell migration and cell area observed after treatment, the number of focal adhesions per cell was analysed. In MCF7 cells, dox treatment led to a significant increase in the number of FA per cell ($p < 0.05$), while other conditions had no effect (Fig. 7A, B). Dox also increased the number of FA in MDA-MB-231 cells ($p < 0.01$, Fig. 7C, D). The increase was more evident in cells co-treated with dox and MnP ($p < 0.001$ versus control), suggesting a possible mechanistic link between the observed changes in cell area and in the number of FA. While treatment of MCF7 cells with dox + MnP only increased the number of focal adhesions by 7% when compared with control, an increase of 37% was observed in MDA-MB-231. Comparing the impact of this treatment in both cell lines, a significantly

difference was clear ($p < 0.001$).

3.7. Impact of MnTnHex-2-PyP and dox on the expression of focal adhesion proteins

Since the drug treatments altered the number of FA, the levels of several proteins involved in the focal adhesion complexes were evaluated by immunoblotting (IB). For both cell lines, the exposure to dox and/or MnP did not significantly alter the levels of FAK, pFAK, vinculin, and paxillin (Fig. 8).

3.8. Impact of MnTnHex-2-PyP and dox on NF- κ B activation

Alterations in intracellular levels of H_2O_2 modulate various signaling pathways, such as NF- κ B [32]. This transcription factor is highly relevant for cell migration and invasion [33–36]. NF- κ B activation upon treatment with dox and/or MnP was evaluated using a luciferase-based gene reporter assay. In MCF7 cells, dox and MnP alone increased NF- κ B activation by approximately 2-fold, while the co-treatment led to a reduction to levels similar to those of non-treated cells (Fig. 9A). In MDA-MB-231 cells, dox and MnP, per se, did not change NF- κ B activation. Conversely, the combined treatment led to a significant increase (Fig. 9B). This finding is in accordance with the study of Shah et al. [37], who demonstrated that the addition of an MnP to MDA-MB-231 enhanced H_2O_2 levels leading to an increase in NF- κ B activity.

4. Discussion

SODm are currently being tested in different clinical trials, in combination with chemo- or radiotherapy, due to their capability of boosting anticancer treatments, while protecting non-tumor tissues from ROS-mediated side effects [4]. However, only very scarce data is available regarding the impact of SODm in cell migration and invasion, which are determinant features of cancer progression and prognosis. Regarding native SOD enzymes, their effects in cancer metastases are still unclear. In many conditions, including advanced breast cancer, SOD seems to promote cancer progression and aggressiveness [5,6]. This fact raises some concerns on the use of SODm in cancer treatment, justifying the need to comprehend the effects of SODm in cellular processes related to the formation of metastases.

O'Leary et al. [38] showed that the SODm GC4419 significantly decreases the invasive capacity of pancreatic ductal adenocarcinoma cells. Tong et al. [39] have shown that MnTE-2-PyP (30 μ M) reduced the migration and invasion of prostate cancer cells. Recently, an in vivo study conducted by Chatterjee et al. [40] showed that MnTE-2-PyP did not affect the metastatic progression of PC3 cells in an orthotopic prostate tumor model. On the other hand, in a mouse D-245MG glioma xenograft model, down-regulation of metastatic pathways was observed upon treatment with MnP + radiation vs radiation only [41]. Regarding breast cancer, our group has previously shown that a macrocyclic copper(II) complex with superoxide scavenger activity decreased MCF7-directed cell migration and, in combination with dox, reduced the invasion of MDA-MB-231 cells [22]. Shah et al. [37] reported that the SODm EUK134 reduced the adhesion of MDA-MB-21 cells and the chemotaxis of MCF7 and MDA-MB-231 cells. However, these results were observed at cytotoxic concentrations of EUK134. In the same report, MnTM-4-PyP was also studied. This MnP decreased the adhesion and enhanced the chemotaxis of MDA-MB-231 cells, while in MCF7 only a minor decrease in chemotactic migration was observed [37].

The few available studies are insufficient to draw conclusions on the impact of SODm in breast cancer metastases. Therefore, we herein studied the potential impact of the SODm MnTnHex-2-PyP in cancer cells migration in the breast cancer models MCF-7 (non-invasive) and MDA-MB-231 cells (invasive). Importantly, these studies were carried out at concentrations that did not impair cell viability. Although the use of low concentrations may lead to less pronounced effects, this is a

technical requirement for an accurate evaluation of changes in the migratory phenotype, excluding the influence of cytotoxicity. Moreover, the concentrations used in this work are biologically relevant. A pharmacokinetic study of this MnP carried out in mice found plasma and tissue concentrations in the order of magnitude of low micromolar [19]. Regarding dox, the concentration used herein is in the range of steady-state plasma concentrations (25–250 nM) observed in patients after standard bolus infusion [20,21].

In this work, the intracellular ROS levels observed are compatible with the SOD-like activity of MnP. MnP decreased superoxide and increased H₂O₂, which is in accordance with previous studies [37,39]. Cells co-treated with MnP and dox showed increased ROS levels, at least partially due to an increase in H₂O₂. Previous studies have suggested that both O₂^{•-} and H₂O₂ are relevant for the regulation of cell migration [33]. While H₂O₂ seems to be a key signaling molecule in this process, the exact impact of H₂O₂ is still unknown and may vary with the cell type, concentrations, and specific conditions, justifying the contradictory reports found in the literature [42–45]. As different types of cell migration have been described in breast cancer [46,47], our study also addressed different types of cell migration. The MnP, when used as a single agent, did not impact on collective, chemotactic or random cell migration. Regarding dox, an increase in random migration was observed, along with an increase in the number of focal adhesions. Although contradictory data can be found in the literature [31,48,49], several reports demonstrate that dox might promote migratory and invasive phenotypes. Regarding breast cancer, Bandyopadhyay et al. [50] have described that dox increased cell migration and invasion in breast cancer cells, and it induced lung metastasis of human breast cancer cells. In addition, Niu et al. [36] observed a marked increase in MDA-MB-231 cells migration and invasiveness upon treatment with dox. These effects might be critical in cells that contact with lower drug concentrations and therefore remain viable after chemotherapy. Importantly, we herein showed that the addition of MnP counteracted most of the dox-induced effects, suggesting potential clinical benefits of combining dox with MnP. In other endpoints, MnP and dox showed a synergistic effect. Comparing with non-treated cells, the co-treatment with dox and MnP exhibited beneficial effects by reducing collective cell migration and chemotaxis. These differences might be partially explained by the alterations detected in cell area and FA number. Cell invasion is a particular type of cell migration particularly relevant in the metastatization process. The drugs under study reduced proteolytic MDA-MB-231 cell invasion, especially in combination.

NF-κB is a redox-regulated transcription factor, highly relevant for cell migration and invasion [33–36]. Previous studies showed that MnP can modulate NF-κB activity [41] by a direct pro-oxidative effect in this transcription factor subunits that affects DNA-binding properties [51], but also indirectly by increasing H₂O₂ production [37]. The dose-dependence and the exact mechanism behind NF-κB regulation by MnPs are still under investigation. H₂O₂ cannot be simply defined as a NF-κB inducer but should instead be considered as a fine-tuning modulator of NF-κB activation pathway by other agents [32]. The differential results observed in the two cell lines may be attributed to the inherent differences in peroxide levels and in antioxidant enzymes of MCF7 and MDA-MB-231 cells [22,52,53]. Moreover, in the MDA-MB-231 cells, NF-κB is constitutively activated, contributing to the aggressive phenotype of these cells [54,55].

Although we have obtained differential results, depending on cell line and migration type, the alterations induced by MnP in dox-treated cells were consistently towards a therapeutically favorable effect on cell phenotype. These data contribute to substantiate the usefulness and safety of SODm-based treatments in breast cancer therapy.

Acknowledgments

This work was financially supported by Fundação para a Ciência e a Tecnologia (FCT, Portugal), through funding UID/DTP/04567/2016 to

CBIOS and funding UID/DTP/04138/2013, to iMed.Ulisboa. Nuno Almeida acknowledges his research grant attributed in the scope of the project UID/DTP/04567/2016. João Costa acknowledges his research grant PADDIC 2016–2017, awarded by Associação Lusófona para o Desenvolvimento da Investigação e Ensino em Ciências da Saúde - Cooperativa de Formação e Animação Cultural crl (ALIES-COFAC, Portugal). Authors also acknowledge the European Cooperation in Science and Technology (COST, European Union) action BM1203 EU-ROS.

References

- [1] I. Batinic-Haberle, A. Tovmasyan, I. Spasojevic, An educational overview of the chemistry, biochemistry and therapeutic aspects of Mn porphyrins - from superoxide dismutation to H₂O₂-driven pathways, *Redox Biol.* 5 (2015) 43–65, <https://doi.org/10.1016/j.redox.2015.01.017>.
- [2] I. Batinic-Haberle, I. Spasojevic, Complex chemistry and biology of redox-active compounds, commonly known as SOD mimics, affect their therapeutic effects, *Antioxid. Redox Signal.* 20 (2014) 2323–2325, <https://doi.org/10.1089/ars.2014.5921>.
- [3] I. Batinic-Haberle, J.S. Rebouças, I. Spasojevic, Superoxide dismutase mimics: chemistry, pharmacology, and therapeutic potential, *Antioxid. Redox Signal.* 13 (2010) 877–918, <https://doi.org/10.1089/ars.2009.2876>.
- [4] J. Egea, I. Fabregat, Y.M. Frapart, P. Ghezzi, A. Görlach, T. Kietzmann, K. Kubaichuk, U.G. Knaus, M.G. Lopez, G. Olaso-Gonzalez, A. Petry, R. Schulz, J. Vina, P. Winyard, K. Abbas, O.S. Ademowo, C.B. Afonso, I. Andreadou, H. Antelmans, F. Antunes, M. Aslan, M.M. Bachschmid, R.M. Barbosa, V. Belousov, C. Berndt, D. Bernlohr, E. Bertrán, A. Bindoli, S.P. Bottari, P.M. Brito, G. Carrara, A.I. Casas, A. Chatzi, N. Chondrogianni, M. Conrad, M.S. Cooke, J.G. Costa, A. Cuadrado, P. My-Chan Dang, B. De Smet, B. Debelec-Butuner, I.H.K. Dias, J.D. Dunn, A.J. Edson, M. El Assar, J. El-Benna, P. Ferdinandy, A.S. Fernandes, K.E. Fladmark, U. Förstermann, R. Giniatullin, Z. Giricz, A. Görbe, H. Griffiths, V. Hampl, A. Hanf, J. Herget, P. Hernansanz-Agustín, M. Hillion, J. Huang, S. Ilikay, P. Jansen-Dürr, V. Jaquet, J.A. Joles, B. Kalyanaraman, D. Kaminsky, M. Karbaschi, M. Kleanthous, L.-O. Klotz, B. Korac, K.S. Korkmaz, R. Koziel, D. Kračun, K.-H. Krause, V. Křen, T. Krieg, J. Laranjinha, A. Lazou, H. Li, A. Martínez-Ruiz, R. Matsui, G.J. McBean, S.P. Meredith, J. Messens, V. Miguel, Y. Mikhed, I. Milisav, L. Milković, A. Miranda-Vizuete, M. Mojović, M. Monsalve, P.-A. Mouthuy, J. Mulvey, T. Münzel, V. Muzykantov, I.T.N. Nguyen, M. Oelze, N.G. Oliveira, C.M. Palmeira, N. Papaevgeniou, A. Pavićević, B. Pedre, F. Peyrot, M. Phylactides, G.G. Pircalabioru, A.R. Pitt, H.E. Poulsen, I. Prieto, M.P. Rigobello, N. Robledinos-Antón, L. Rodríguez-Mañas, A.P. Rolo, F. Rousset, T. Ruskovska, N. Saraiva, S. Sasson, K. Schröder, K. Semen, T. Seredenina, A. Shakirzyanova, G.L. Smith, T. Soldati, B.C. Sousa, C.M. Spickett, A. Stancic, M.J. Stasia, H. Steinbrenner, V. Stepanić, S. Steven, K. Tokatlidis, E. Tuncay, B. Turan, F. Ursini, J. Vacek, O. Vajnerova, K. Valentová, F. Van Breusegem, L. Varisli, E.A. Veal, A.S. Yalçın, O. Yelisseyeva, N. Žarković, M. Zatloukalová, J. Zielonka, R.M. Touyz, A. Papapetropoulos, T. Grune, S. Lamas, H.H.H.W. Schmidt, F. Di Lisa, A. Daiber, European contribution to the study of ROS: a summary of the findings and prospects for the future from the cost action BM1203 (EU-ROS), *Redox Biol.* 13 (2017) 94–162, <https://doi.org/10.1016/j.redox.2017.05.007>.
- [5] A.S. Fernandes, N. Saraiva, N.G. Oliveira, Redox therapeutics in breast cancer: role of SOD mimics, in: I. Batinic-Haberle, J.S. Rebouças, I. Spasojevic (Eds.), *Redox-Active Therapeutics*, 2016, pp. 451–467, https://doi.org/10.1007/978-3-319-30705-3_18.
- [6] V.L. Kinnula, J.D. Crapo, Superoxide dismutases in malignant cells and human tumors, *Free Radic. Biol. Med.* 36 (2004) 718–744, <https://doi.org/10.1016/j.freeradbiomed.2003.12.010>.
- [7] L.W. Oberley, Mechanism of the tumor suppressive effect of MnSOD over-expression, *Biomed. Pharmacother.* 59 (2005) 143–148, <https://doi.org/10.1016/j.biopha.2005.03.006>.
- [8] N. Hempel, P.M. Carrico, J.A. Melendez, Manganese superoxide dismutase (Sod2) and redox-control of signaling events that drive metastasis, *Anticancer. Agents Med. Chem.* 11 (2011) 191–201.
- [9] I. Batinic-Haberle, I. Spasojevic, R.D. Stevens, P. Hambright, I. Fridovich, Manganese(III) meso-tetrakis(ortho-N-alkylpyridyl)porphyrins. Synthesis, characterization, and catalysis of O₂^{•-} dismutation, *J. Chem. Soc. Dalton Trans.* (2002) 2689, <https://doi.org/10.1039/b201057g>.
- [10] A.S. Fernandes, J. Gaspar, M.F. Cabral, J. Rueff, M. Castro, I. Batinic-Haberle, J. Costa, N.G. Oliveira, Protective role of ortho-substituted Mn(III) N-alkylpyridylporphyrins against the oxidative injury induced by tert-butylhydroperoxide, *Free Radic. Res.* 44 (2010) 430–440, <https://doi.org/10.3109/10715760903555844>.
- [11] L. Bellner, L. Martinelli, A. Halilovic, K. Patil, N. Puri, M.W. Dunn, R.F. Regan, M.L. Schwartzman, Heme oxygenase-2 deletion causes endothelial cell activation marked by oxidative stress, inflammation, and angiogenesis, *J. Pharmacol. Exp. Ther.* 331 (2009) 925–932, <https://doi.org/10.1124/jpet.109.158352>.
- [12] O. Handa, Y. Naito, T. Takagi, M. Shimozawa, S. Kokura, N. Yoshida, H. Matsui, G. Cepinskas, P.R. Kvietys, T. Yoshikawa, Tumor necrosis factor-α-induced cytokine-induced neutrophil chemoattractant-1 (CINC-1) production by rat gastric epithelial cells: role of reactive oxygen species and nuclear factor-κB, *J. Pharmacol. Exp. Ther.* 309 (2004) 670–676, <https://doi.org/10.1124/jpet.103.062216>.

- [13] C.A. Schneider, W.S. Rasband, K.W. Eliceiri, NIH Image to ImageJ: 25 years of image analysis, *Nat. Methods* 9 (2012) 671–675.
- [14] C.-C. Liang, A.Y. Park, J.-L. Guan, In vitro scratch assay: a convenient and inexpensive method for analysis of cell migration in vitro, *Nat. Protoc.* 2 (2007) 329–333, <https://doi.org/10.1038/nprot.2007.30>.
- [15] A. Albini, R. Benelli, The chemoinvasion assay: a method to assess tumor and endothelial cell invasion and its modulation, *Nat. Protoc.* 2 (2007) 504–511, <https://doi.org/10.1038/nprot.2006.466>.
- [16] A. Albini, D.M. Noonan, The “chemoinvasion” assay, 25 years and still going strong: the use of reconstituted basement membranes to study cell invasion and angiogenesis, *Curr. Opin. Cell Biol.* 22 (2010) 677–689, <https://doi.org/10.1016/j.ccb.2010.08.017>.
- [17] N. Saraiva, D.L. Prole, G. Carrara, B.F. Johnson, C.W. Taylor, M. Parsons, G.L. Smith, HGAP promotes cell adhesion and migration via the stimulation of store-operated Ca²⁺ entry and calpain 2, *J. Cell Biol.* 202 (2013) 699–713, <https://doi.org/10.1083/jcb.201301016>.
- [18] K.H. Martin, K.E. Hayes, E.L. Walk, A.G. Ammer, S.M. Markwell, S.A. Weed, Quantitative measurement of invadopodia-mediated extracellular matrix proteolysis in single and multicellular contexts, *J. Vis. Exp.* (2012) 1–10, <https://doi.org/10.3791/4119>.
- [19] T. Weitner, I. Kos, H. Sheng, A. Tovmasyan, J.S. Reboucas, P. Fan, D.S. Warner, Z. Vujaskovic, I. Batinic-Haberle, I. Spasojevic, Comprehensive pharmacokinetic studies and oral bioavailability of two Mn porphyrin-based SOD mimics, MnTE-2-PyP5+ and MnTnHex-2-PyP5+, *Free Radic. Biol. Med.* 58 (2013) 73–80, <https://doi.org/10.1016/j.freeradbiomed.2013.01.006>.
- [20] G. Minotti, Anthracyclines: molecular advances and pharmacologic developments in antitumor activity and cardiotoxicity, *Pharmacol. Rev.* 56 (2004) 185–229, <https://doi.org/10.1124/pr.56.2.6>.
- [21] D.A. Gewirtz, A critical evaluation of the mechanisms of action proposed for the antitumor effects of the anthracycline antibiotics adriamycin and daunorubicin, *Biochem. Pharmacol.* 57 (1999) 727–741, [https://doi.org/10.1016/S0006-2952\(98\)00307-4](https://doi.org/10.1016/S0006-2952(98)00307-4).
- [22] A.S. Fernandes, A. Flório, N. Saraiva, S. Cerqueira, S. Ramalhet, M. Cipriano, M.F. Cabral, J.P. Miranda, M. Castro, J. Costa, N.G. Oliveira, Role of the copper(II) complex Cu[15]pyN5 in Intracellular ROS and breast cancer cell motility and invasion, *Chem. Biol. Drug Des.* 86 (2015) 578–588, <https://doi.org/10.1111/cbdd.12521>.
- [23] F. Foroodi, W.C. Duivenvoorden, G. Singh, Interactions of doxycycline with chemotherapeutic agents in human breast adenocarcinoma MDA-MB-231 cells, *Anticancer Drugs* 20 (2009) 115–122, <https://doi.org/10.1097/CAD.0b013e32831c14ec>.
- [24] P. Wardman, Fluorescent and luminescent probes for measurement of oxidative and nitrosative species in cells and tissues: progress, pitfalls, and prospects, *Free Radic. Biol. Med.* 43 (2007) 995–1022, <https://doi.org/10.1016/j.freeradbiomed.2007.06.026>.
- [25] A.S. Fernandes, J. Serejo, J. Gaspar, F. Cabral, A.F. Bettencourt, J. Rueff, M. Castro, J. Costa, N.G. Oliveira, Oxidative injury in V79 Chinese hamster cells: protective role of the superoxide dismutase mimetic MnTM-4-PyP, *Cell Biol. Toxicol.* 26 (2010) 91–101, <https://doi.org/10.1007/s10565-009-9120-3>.
- [26] S. Gonçalves, A.S. Fernandes, N.G. Oliveira, J. Marques, J. Costa, M. Fátima Cabral, J. Miranda, M. Cipriano, P.S. Guerreiro, M. Castro, Cytotoxic effects of cadmium in mammary epithelial cells: protective role of the macrocycle [15]pyN5, *Food Chem. Toxicol.* 50 (2012) 2180–2187, <https://doi.org/10.1016/j.fct.2012.04.006>.
- [27] J.G. Costa, N. Saraiva, P.S. Guerreiro, H. Louro, M.J. Silva, J.P. Miranda, M. Castro, I. Batinic-Haberle, A.S. Fernandes, N.G. Oliveira, Ochratoxin A-induced cytotoxicity, genotoxicity and reactive oxygen species in kidney cells: an integrative approach of complementary endpoints, *Food Chem. Toxicol.* 87 (2016) 65–76, <https://doi.org/10.1016/j.fct.2015.11.018>.
- [28] J.M. Berthiaume, K.B. Wallace, Adriamycin-induced oxidative mitochondrial cardiotoxicity, *Cell Biol. Toxicol.* 23 (2007) 15–25, <https://doi.org/10.1007/s10565-006-0140-y>.
- [29] Q. Lv, W. Wang, J. Xue, F. Hua, R. Mu, H. Lin, J. Yan, X. Lv, X. Chen, Z.W. Hu, DEDD interacts with PI3K3 to activate autophagy and attenuate epithelial-mesenchymal transition in human breast cancer, *Cancer Res.* 72 (2012) 3238–3250, <https://doi.org/10.1158/0008-5472.CAN-11-3832>.
- [30] F. Sabeh, R. Shimizu-Hirota, S.J. Weiss, Protease-dependent versus-independent cancer cell invasion programs: three-dimensional amoeboid movement revisited, *J. Cell Biol.* 185 (2009) 11–19, <https://doi.org/10.1083/jcb.200807195>.
- [31] E.H. Mustafa, H.T. Mahmoud, M.Y. Al-Hudhud, M.Y. Abdalla, I.M. Ahmad, S.R. Yasin, A.Z. Elkarmi, L.H. Tahtamouni, 2-deoxy-D-glucose synergizes with doxorubicin or L-buthionine sulfoximine to reduce adhesion and migration of breast cancer cells, *Asian Pac. J. Cancer Prev.* 16 (2015) 3213–3222, <https://doi.org/10.7314/APJCP.2015.16.8.3213>.
- [32] V. de Oliveira-Marques, L. Cyrne, H.S. Marinho, F. Antunes, A quantitative study of NF-kappaB activation by H₂O₂: relevance in inflammation and synergy with TNF-alpha, *J. Immunol.* 178 (2007) 3893–3902, <https://doi.org/10.4049/jimmunol.178.6.3893>.
- [33] T.R. Hurd, M. DeGennaro, R. Lehmann, Redox regulation of cell migration and adhesion, *Trends Cell Biol.* 22 (2012) 107–115, <https://doi.org/10.1016/j.tcb.2011.11.002>.
- [34] A. Adhikary, S. Mohanty, L. Lahiry, D.M.S. Hossain, S. Chakraborty, T. Das, Theaflavins retard human breast cancer cell migration by inhibiting NF-κB via p53-ROS cross-talk, *FEBS Lett.* 584 (2010) 7–14, <https://doi.org/10.1016/j.febslet.2009.10.081>.
- [35] M.J. Morgan, Z. Liu, Crosstalk of reactive oxygen species and NF-κB signaling, *Cell Res.* 21 (2011) 103–115, <https://doi.org/10.1038/cr.2010.178>.
- [36] J. Niu, Y. Shi, G. Tan, C.H. Yang, M. Fan, L.M. Pfeffer, Z.H. Wu, DNA damage induces NF-κB-dependent MicroRNA-21 up-regulation and promotes breast cancer cell invasion, *J. Biol. Chem.* 287 (2012) 21783–21795, <https://doi.org/10.1074/jbc.M112.355495>.
- [37] M.H. Shah, G.S. Liu, E.W. Thompson, G.J. Dusting, H.M. Peshavariya, Differential effects of superoxide dismutase and superoxide dismutase/catalase mimetics on human breast cancer cells, *Breast Cancer Res. Treat.* 150 (2015) 523–534, <https://doi.org/10.1007/s10549-015-3329-z>.
- [38] B.R. O’Leary, M.A. Fath, A.M. Bellizzi, J.E. Hrabe, A.M. Button, B.G. Allen, A.J. Case, S. Altekruze, B.A. Wagner, G.R. Buettner, C.F. Lynch, B.Y. Hernandez, W. Cozen, R.A. Beardsley, J. Keene, M.D. Henry, F.E. Domann, D.R. Spitz, J.J. Mezhir, Loss of SOD3 (EcsOD) expression promotes an aggressive phenotype in human pancreatic ductal adenocarcinoma, *Clin. Cancer Res.* 21 (2015) 1741–1751, <https://doi.org/10.1158/1078-0432.CCR-14-1959>.
- [39] Q. Tong, M.R. Weaver, E.A. Kosmacek, B.P. O’Connor, L. Harmacek, S. Venkataraman, R.E. Oberley-Deegan, MnTE-2-PyP reduces prostate cancer growth and metastasis by suppressing p300 activity and p300/HIF-1/CREB binding to the promoter region of the PAI-1 gene, *Free Radic. Biol. Med.* 94 (2016) 185–194, <https://doi.org/10.1016/j.freeradbiomed.2016.02.036>.
- [40] A. Chatterjee, Y. Zhu, Q. Tong, E. Kosmacek, E. Lichter, R. Oberley-Deegan, The addition of manganese porphyrins during radiation inhibits prostate cancer growth and simultaneously protects normal prostate tissue from radiation damage, *Antioxidants* 7 (2018) 21, <https://doi.org/10.3390/antiox7010021>.
- [41] I. Batinic-Haberle, A. Tovmasyan, I. Spasojevic, Mn porphyrin-based redox-active drugs – differential effects as cancer therapeutics and protectors of normal tissue against oxidative injury, *Antioxid. Redox Signal.* (2018), <https://doi.org/10.1089/ars.2017.7453>.
- [42] A.Y. Alexandrova, P.B. Kopnin, J.M. Vasiliev, B.P. Kopnin, ROS up-regulation mediates Ras-induced changes of cell morphology and motility, *Exp. Cell Res.* 312 (2006) 2066–2073, <https://doi.org/10.1016/j.yexcr.2006.03.004>.
- [43] F. Li, H. Wang, C. Huang, J. Lin, G. Zhu, R. Hu, H. Feng, Hydrogen peroxide contributes to the manganese superoxide dismutase promotion of migration and invasion in glioma cells, *Free Radic. Res.* 45 (2011) 1154–1161, <https://doi.org/10.3109/10715762.2011.604321>.
- [44] C. Polyarchou, M. Hatzia Apostolou, E. Papadimitriou, Hydrogen peroxide stimulates proliferation and migration of human prostate cancer cells through activation of activator protein-1 and up-regulation of the heparin affinity regulatory peptide gene, *J. Biol. Chem.* 280 (2005) 40428–40435, <https://doi.org/10.1074/jbc.M505120200>.
- [45] E.L. Reineke, Y. Liu, H.-Y. Kao, Promyelocytic leukemia protein controls cell migration in response to hydrogen peroxide and insulin-like growth factor-1, *J. Biol. Chem.* 285 (2010) 9485–9492, <https://doi.org/10.1074/jbc.M109.063362>.
- [46] P. Friedl, K. Wolf, Tumour-cell invasion and migration: diversity and escape mechanisms, *Nat. Rev. Cancer* 3 (2003) 362–374, <https://doi.org/10.1038/nrc1075>.
- [47] A.G. Clark, D.M. Vignjevic, Modes of cancer cell invasion and the role of the microenvironment, *Curr. Opin. Cell Biol.* 36 (2015) 13–22, <https://doi.org/10.1016/j.ccb.2015.06.004>.
- [48] G. Brum, T. Carbone, E. Still, V. Correia, K. Szulak, D. Calianese, C. Best, G. Cammarata, K. Higgins, F. Ji, W. Di, Y. Wan, N-acetylcysteine potentiates doxorubicin-induced ATM and p53 activation in ovarian cancer cells, *Int. J. Oncol.* 42 (2013) 211–218, <https://doi.org/10.3892/ijo.2012.1680>.
- [49] R. Han, J. Xiong, R. Xiao, E. Altaf, J. Wang, Y. Liu, H. Xu, Q. Ding, Q. Zhang, Activation of β-catenin signaling is critical for doxorubicin-induced epithelial-mesenchymal transition in BGC-823 gastric cancer cell line, *Tumor Biol.* 34 (2013) 277–284, <https://doi.org/10.1007/s13277-012-0548-3>.
- [50] A. Bandyopadhyay, L. Wang, J. Agyin, Y. Tang, S. Lin, I.T. Yeh, K. De, L.Z. Sun, Doxorubicin in combination with a small TGFβ inhibitor: a potential novel therapy for metastatic breast cancer in mouse models, *PLoS One* 5 (2010), <https://doi.org/10.1371/journal.pone.0010365>.
- [51] I. Batinic-Haberle, I. Spasojevic, H.M. Tse, A. Tovmasyan, Z. Rajic, D.K. Clair St., Z. Vujaskovic, M.W. Dewhirst, J.D. Piganelli, Design of Mn porphyrins for treating oxidative stress injuries and their redox-based regulation of cellular transcriptional activities, *Amino Acids* 42 (2012) 95–113, <https://doi.org/10.1007/s00726-010-0603-6>.
- [52] T.C. Hsieh, S. Elangovan, J.M. Wu, Differential suppression of proliferation in MCF-7 and MDA-MB-231 breast cancer cells exposed to α-, γ- and δ-tocotrienols is accompanied by altered expression of oxidative stress modulatory enzymes, *Anticancer Res.* 30 (2010) 4169–4176.
- [53] Z. Kattan, V. Minig, P. Leroy, M. Dauça, P. Becuwe, Role of manganese superoxide dismutase on growth and invasive properties of human estrogen-independent breast cancer cells, *Breast Cancer Res. Treat.* 108 (2008) 203–215, <https://doi.org/10.1007/s10549-007-9597-5>.
- [54] R. Romieu-Mourez, E. Landesman-Bollag, D.C. Seldin, A.M. Traish, F. Mercurio, G.E. Sonenshein, Roles of IKK kinases and protein kinase CK2 in activation of nuclear factor-kappaB in breast cancer, *Cancer Res.* 61 (2001) 3810–3818.
- [55] H. Nakshatri, P. Bhat-Nakshatri, D.A. Martin, R.J.J. Goulet, G.W.J. Sledge, Constitutive activation of NF-kappaB during progression of breast cancer to hormone-independent growth, *Mol. Cell. Biol.* 17 (1997) 3629–3639.